# Review on islanding detection methods for grid-connected photovoltaic systems, existing limitations and future insights

Bakhshi-Jafarabadi, Reza; Sadeh, Javad; Serrano-Fontova, Alexandre; Rakhshani, Elyas

**DOI**
10.1049/rpg2.12554

**Publication date**
2022

**Document Version**
Final published version

**Published in**
IET Renewable Power Generation

Received: 27 February 2022 | Revised: 6 May 2022 | Accepted: 6 July 2022

DOI: 10.1049/rpg2.12554

IET Renewable Power Generation

The Institution of Engineering and Technology WILEY

REVIEW

# Review on islanding detection methods for grid-connected photovoltaic systems, existing limitations and future insights

**Reza Bakhshi-Jafarabadi**[1] | **Javad Sadeh**[1] | **Alexandre Serrano-Fontova**[2] | **Elyas Rakhshani**[3]

[1]Department of Electrical Engineering, Ferdowsi University of Mashhad, Mashhad, Iran

[2]School of Electrical and Electronic Engineering, The University of Manchester, Manchester, UK

[3]Faculty of EEMCS, Delft University of Technology, Delft, The Netherlands

**Correspondence**
Javad Sadeh, Department of Electrical Engineering, Ferdowsi University of Mashhad, Mashhad, Iran.
Email: sadeh@um.ac.ir

**Abstract**

The connection of renewable energy sources (RESs) to the distribution network has been rising at a steady pace over the past decades. The great penetration of RESs such as grid-connected photovoltaic system brings new technical challenges to the distribution networks such as unintentional islanding. Conceptually, this situation occurs when a portion of the network that has been isolated from the main grid remains energised by the embedded RESs. This unexpected scenario should be thereby identified effectively to avoid frequency and voltage deviations and their hazardous effects. The aim of this paper is to provide a comprehensive review on the recently developed islanding detection methods for grid-following/grid-connected photovoltaic system, analyse their existing limitations, and suggest possible future research implementations. In this context, an in-depth comparison is provided considering the main features used in islanding detection methods such as non-detection zone, detection time, implementation cost and complexity, and power quality degradation. Finally, the main technical requirements established by the current grid codes are recalled identifying potential multi-functional approaches to expand the current islanding detection capabilities.

## 1 | INTRODUCTION

In the recent years, renewable energy sources (RESs) have been widely exploited in electrical power systems to mitigate global warming and its hazardous effects. Among all existing technologies, grid-connected photovoltaic system (GCPVS) is gaining prominence due to its various benefits for users and distribution system operators. On the user side, the simple operation, the reduction of the energy trading with the main grid, and its competitive installation costs are the main advantages [1]. From the grid side, the stronger points are efficiency and reliability reinforcement [2].

Similar to other distributed generations (DGs), the interconnection of GCPVSs pose several challenges to the distribution networks (DNs), such as the unintentional islanding operation. This hazardous situation takes place when a microgrid containing both DG(s) and local load is disconnected from the upstream grid by opening the circuit breaker (CB) at the point of common coupling (PCC), as shown in Figure 1 [3–5]. This undesired situation may include power quality (PQ) disturbances such as frequency and voltage deviations, a safety hazard for the network personnel as it is assumed the islanded area is being de-energised, unexpected changes in the fault current level as a consequence of the shift in the earthing system and a damaging effect on electrical machines and transformers due to the out-of-phase reclosing [6]. Considering these aforementioned drawbacks, preventing such conditions and keeping the grid operating safely becomes mandatory. In this context, IEEE Std. 1547–2018 and UL 1741 propose a procedure to be followed in the islanding operating mode and suggest a maximum time of 2 s for ceasing/controlling the DG generation [7, 8]. A common option for constructing a power plant GCPVS is to deploy numerous series of multi-string inverters in parallel, e.g., typically within the range of 50–200 kW nominal output power). Therefore, an effective islanding protection should also tackle the effects of such a practical scenario.

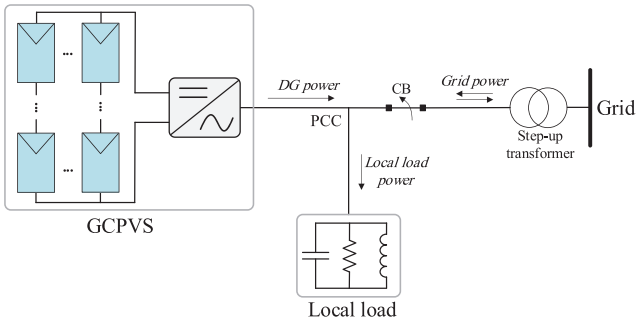


**FIGURE 1** Typical scheme of a GCPVS with parallel RLC load

Several islanding detection methods (IDMs) have been presented in the literature, categorised into four main groups: communication-based, passive, active, and hybrid methods [3–5]. The first type relies basically on broadband technologies such as optic-fibre and power line communications for establishing direct communication between the CB of the substation-feeder and the CB located at the DG interconnection bus. Albeit several communication protocols can be established, the islanding mode is normally identified quickly after the operation of the CB between the upstream grid and DG(s) path [9–13]. Although these schemes are known as the most reliable islanding classifiers for both inverter- and synchronous-based technologies, the expensive structure limits its practical implementation in small-scale DGs such as residential GCPVSs [14].

Passive algorithms use the local measurements acquired at the PCC. In the traditional passive IDMs, time-domain variables are continuously measured and compared to a pre-set threshold [15, 16]. After the island formation, as the main grid is no longer dictating both voltage and frequency, the variables are shifted into a new state according to the mismatch between generation and load. In most cases, this mismatch is large enough for the timeliness shifting of the mentioned state variables beyond the pre-set thresholds. Nevertheless, the worst scenario occurs when negligible power flows to/from the grid and state variables barely deviate from their rated values. The thresholds of the passive IDMs are thereby assigned eminently small to identify these challenging scenarios. However, this tuning process may cause false operation during some non-islanding events that imply either voltage or frequency deviations, e.g. short-circuit faults, capacitor bank, load/induction motor switching, and transformer energisation. Therefore, optimum thresholds determination is known as the main challenge of the passive IDMs to achieve minimum false tripping in non-islanding incidents and minimum non-detection zone (NDZ), i.e. the cases wherein the employed technique fails to recognise islanding. Frequency-based [17] and pattern recognition techniques [18] have been recently established to mitigate the NDZ of the traditional time-domain passive-based protection relays. Although these IDMs distinguish islanding and non-islanding states reliably through employing computationally advanced techniques, the high dependency of the threshold settings on the type/size of the DG/network under study is known as their main demerit.

In active techniques, a controlled disturbance is injected into the GCPVS control loop to destabilise a local variable during islanding. Conversely, the effects of the imposed disturbance are negligible in the grid-connected mode as the GCPVS follows the voltage and frequency governed strictly by the upstream network [19]. Although these schemes have reduced the NDZ and detection time substantially with respect to the passive IDMs, the injected disturbance can degrade the PQ during the grid-connected operation.

Finally, both passive and active methodologies are combined in the so-called hybrid IDMs. The disturbance of the active technique is thereby triggered if a passive criterion suspects islanding. Therefore, the NDZ is reduced drastically whilst PQ is barely degraded in the grid-connected operation [20]. The expensive structure and the large detection time are reported as the main limitations of these two-level schemes.

This paper essentially aims to review the recently developed islanding detection methodologies for GCPVS. However, the main contributions of this work are listed as follows:

- Performing a comprehensive analysis of the existing GCPVS-based IDMs.
- Providing a detailed comparison and discussion between algorithms considering the paramount features in islanding detection, including NDZ, detection time, cost and complexity, PQ degradation, and the capability for seamlessly transitioning from grid-connected to the standalone mode.
- Shedding some light on the current limitations of the analysed IDMs, especially when they interact with the ancillary services in the DNs and underscore the future trends of this promising technology.
- Identifying the challenges of the existing IDMs and proposing solutions for future studies and developments.

Most GCPVS-based active/hybrid IDMs have been implemented in the voltage source inverters (VSIs). Hence, the control loops of the VSI are firstly explained in Section 2. Section 3 elaborates on the recent islanding detection developments for GCPVS. The main features of these IDMs are then thoroughly compared in Section 4. Since the GCPVSs will play a significant role in supporting the future DNs by providing ancillary services, the current status of these functionalities and their interaction with IDMs are analysed in Section 5. Finally, Section 6 presents the main advantages and challenges of the existing IDMs and proposes a few recommendations as future lines of research.

## 2 | VOLTAGE SOURCE INVERTER MODELLING FOR ISLANDING DETECTION PURPOSES

The VSI is composed of two independent control loops as illustrated in Figure 2; voltage and current [21]. The voltage control loop tracks the PV array's maximum power point (MPP) in any operating condition, e.g. various irradiance levels and ambient temperatures. This is accomplished by applying search-based

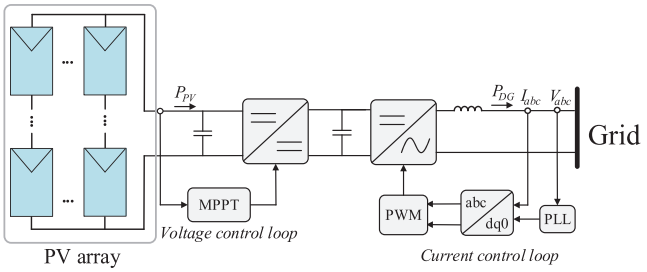


**FIGURE 2** Control loops of the voltage source inverter

and metaheuristic-based MPP tracking (MPPT) algorithms in the DC/DC converter [22]. Further, the current control loop balances the PV array and output power ($P_{PV}$ and $P_{DG}$), synchronises the output current ($I_{ABCabc}$) with the output voltage ($V_{abc}$), and ensures PQ requirements. The first aim is achieved by eliminating the steady-state error between the reference current/power and the measured ones through proportional–integral (PI) and proportional-resonant (PR) controllers in *dq0* and *αβ0* reference frames, respectively [21]. The synchronisation between the output current and voltage is also fulfilled through different techniques such as phase-locked loop (PLL). The reference switching signal of the DC/AC converter is eventually generated to obtain a sinusoidal output current with low harmonic content, i.e. keeping the current total harmonic distortion (THD) below 5% [7, 8]. In this regard, pulse width modulation (PWM) and space vector modulation (SVM) are among the most applied switching techniques.

From the islanding detection standpoint, the dynamic response time of the current controller is fast enough for destabilizing a local variable during an islanding event through a periodic disturbance. Conversely, since the MPPT algorithm is realised at a lower frequency, an open-loop disturbance should be injected to assure enough effect is caused in a local variable so that it deviates from the pre-set limits. Therefore, several active/hybrid IDMs have exploited the current control loop to inject a periodic disturbance while a few techniques used the voltage control loop for this purpose.

## 3 | ISLANDING DETECTION METHODOLOGIES FOR GRID-CONNECTED PHOTOVOLTAIC SYSTEMS

This section describes the recent islanding detection developments for GCPVS. These IDMs can be divided into the remote, passive, active, and hybrid techniques, elaborated as follows and summarised in Figure 3.

### 3.1 | Telecommunication-based methods

The common feature of these techniques essentially lies in connecting the upstream substation and DG(s) through a telecommunication channel given a certain protocol. In the direct transfer trip (DTT) scheme depicted in Figure 4(a), the

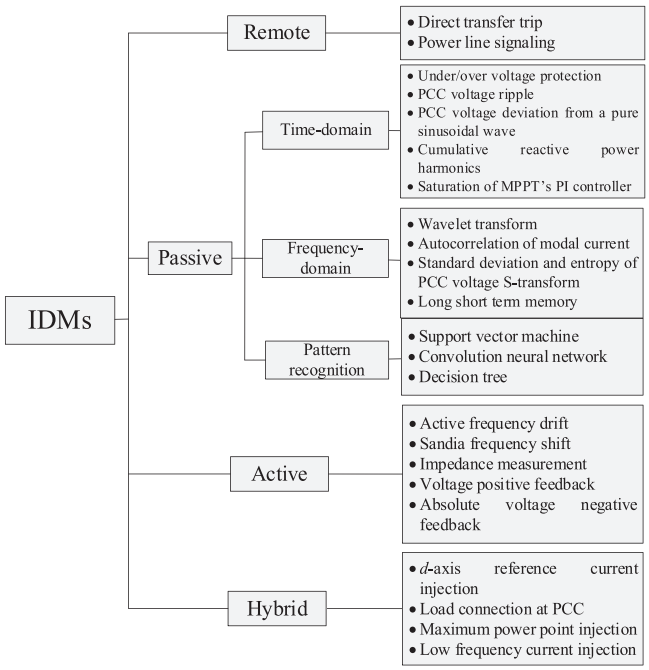


**FIGURE 3** Categorisation of islanding detection methodologies

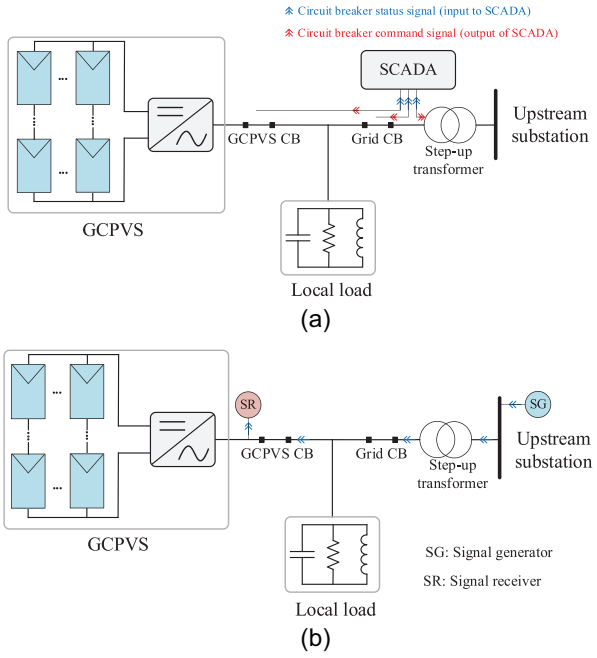


**FIGURE 4** Remote IDMs. (a) Direct transfer trip, (b) power line signalling

status of GCPVSs, CBs, and upstream substation are monitored through supervisory control and data acquisition (SCADA) system. The tripping signal is sent to the CB located at the GCPVSs when the utility SCADA identifies the failed operation of any switching device within the DN that can de-energise the microgrid. It is worthwhile to note that this operation can be motivated by either a grid fault or unscheduled grid reconfiguration [9]. This methodology has been also used by Cataliotti et al. to protect and control a low voltage distribution network [10].

The data of the protection station is sent to the CBs through power line communication. The algorithm provides the chance of voltage regulation of the islanded microgrid as shown in the presented analysis.

In the power line signalling technique illustrated in Figure 4(b), so as to establish communication between the substation and the GCPV CB, a signal generator and a signal receiver are implemented at the main substation and at the GCPV's end, respectively. Thereby, a signal is periodically injected into the grid by the generator and received by the end device. If a switch between the upstream substation and the GCPVS is operated, the communication between devices is lost, and islanding is identified [11].

A distributed communication-based IDM has been established by Ma et al. [12]. The microgrid is firstly divided into several distributed systems, equipped with the intelligent electronic device (IED). The status of the CBs of the distributed systems is then monitored online for islanding classification. The authors employed a topology graph for optimum distributed system definition. The simulation outputs endorsed zero NDZ of the presented scheme with better real-time performance, i.e. detection within 283 ms. Song et al. presented the status of the CBs in a DC distribution network, assisted by a local-based criteria [13]. Islanding condition is detected in case the CB(s) status changes to open. The algorithm is supported through measuring CBs' current and the voltage difference between various nodes. Islanding is recognised when the CB's current and voltage deviation over a given time frame is either near-zero or greater than a threshold, respectively.

These communication-assisted schemes can be integrated into all microgrids, disregarding the technology, size, and number of DG(s), and identify the islanding condition even in a perfect mismatch scenario. However, the high implementation cost is still the main challenge of these IDMs, especially for small-scale DGs such as residential GCPVSs [14]. Moreover, the false tripping in the network reconfiguration cases leads to unnecessary microgrid de-energisation.

## 3.2 | Passive-based methods

### 3.2.1 | Protection relays based on time-domain variables

The effectiveness of the conventional passive-based IDMs lies in the measurement of the local variables at PCC or DG's internal control loops. As shown in Figure 5, these local parameters are compared with pre-established settings. After island formation, the grid cannot compensate for the mismatch between generation and load, shifting the state variables to the new value. For example, the PCC voltage change after islanding can be defined as follows:

$$\Delta V_{\mathrm{PCC}} = \frac{V_{\mathrm{pr}}}{\sqrt{1-\frac{\Delta P}{P_{\mathrm{DG}}}}} - V_{\mathrm{pr}} \tag{1}$$

where, pre-islanding PCC voltage and its shift after island formation are denoted by $V_{\mathrm{pr}}$ and $\Delta V_{\mathrm{PCC}}$, respectively. For a great active power imbalance ($\Delta P$), the PCC voltage deviates from its standard limits, and islanding is identified. For instance, when $\Delta P/P_{\mathrm{DG}}$ is either under or above the [−29.13%, 17.35%] range for $V_{\mathrm{pr}} = 100\%$, the post-islanding voltage is out of the [88%, 110%] range; hence, the under/over voltage protection (UVP/OVP) activates and disconnects DG [15].

Several time-domain passive IDMs have exploited the PCC voltage variation as an islanding detection indicator. Against this backdrop, the difference in the voltage measured at the PCC and pure sinusoidal wave has been adopted by Dubey et al. [23]. In an islanded scenario with a remarkable power mismatch, this variable deviates rapidly from the rated value. The authors employed Fourier–Taylor transformation within a moving window and the least square error method to estimate the output voltage. The results unveiled successful islanding detection in less than 55 ms except for the narrow [−1%, 1%] range of relative active ($\Delta P/P_{\mathrm{DG}}$) and reactive power mismatches ($\Delta Q/P_{\mathrm{DG}}$). The ripple of the PCC voltage of GCPVS has been used by Guha et al. [24]. In this work, islanding is identified when the rate of change of PCC voltage (ROCOV) exceeds a given threshold of 300 ms. An intentional time delay has also been considered to discriminate voltage deviations during transient switching events and islanding. Moreover, when the output current surpasses 125%, short-circuit fault incidents are recognised for de-energizing GCPVS. In ref. [25], a field-programmable gate array (FPGA) implementation of an islanding detection technique has been proposed, where the maxima of superimposed voltage components are used. According to the provided outputs, this IDM identifies the perfectly matched islanding scenarios within 11 ms. However, it seems to have a certain undetectable region by investigating the effect of the settings in the results. Haider et al. exploited cumulative reactive power harmonics (CRPH) of the GCPVS, where the output current and voltage are firstly measured to quantify GCPVS reactive power output [26]. The harmonic spectrum of this reactive power is then estimated through the discrete Kalman filter. The authors displayed that the estimated CRPH of an 80 kW GCPVS surpasses a pre-specified threshold within an operating cycle timeframe in a nearly balanced island. The accuracy of this technique is greater than 95% for both islanding and non-islanding cases. Kamyab and Sadeh defined an adaptive piecewise function of the GCPVS active power reference considering PCC voltage [27]. Through this scheme, the $P_{\mathrm{DG}}$ notably reduces so that the new voltage is likely to be beyond the minimum standard set [7, 8], thus activating the UVP. This piecewise function has been determined taking into account the input power limitation of GCPVS in any operating condition. Further, the slope of the mentioned function has been defined adaptively to support different loading levels. The MATLAB/Simulink simulations endorsed successful islanding detection within 1 s under different power mismatches and load quality factors.

Karimi et al. established a passive IDM for inverter-interfaced DGs using ROCOV and the ratio of the voltage magnitude to the current one at the PCC known as VoI [28]. The voltage data is initially collected by phasor measurement

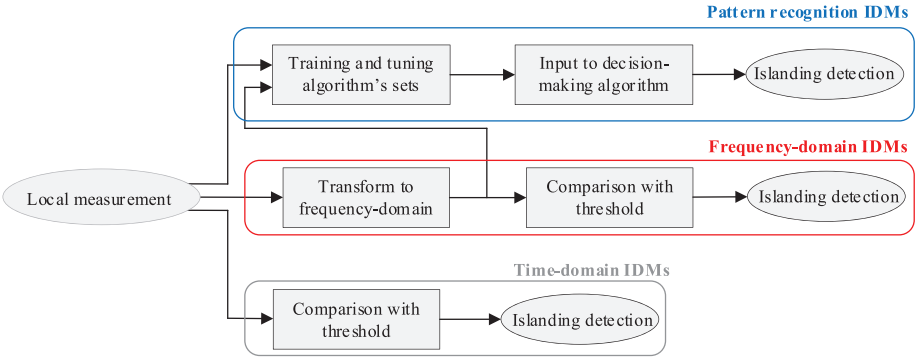


**FIGURE 5** Performance of passive IDMs

units (PMUs), installed at the PCCs, and the ROCOV computed with a 1 kHz sampling frequency. When ROCOV surpasses a certain level, the VoI of each phase is compared with a threshold. The authors claimed that the VoI changes markedly in islanding operation within the [0.1 s, 0.6 s] timeframe, while its variation is hardly appreciable in the non-islanding switching transients. The simulation results for a case study with both GCPVS and other DG technologies demonstrated that the NDZ falls within the narrow [−0.5%, 0.5%] range of the $\Delta P/P_{DG}$ and $\Delta Q/P_{DG}$. This technique has considered a PMU device for each PCC, making it costly. Therefore, it would be economically viable for power plant GCPVS with several parallel VSIs connected to the same bus, thus sharing the PMU unit. In addition, the ROCOV and VoI thresholds have been tuned based on the off-line simulations, which depend largely on the studied test system. Elshrief et al. adopted the rate of change of active power (ROCOP) and PCC voltage deviation for islanding detection purposes [29]. According to the presented MATLAB/Simulink simulations, this technique fails to detect a well-balanced island as the employed variable hardly deviates in such scenarios.

In addition to the PCC electrical quantities, a few researchers focused on the parameters of the VSI's control loops for islanding detection. In the $\alpha\beta 0$ reference frame, the PR controller is exploited to remove the steady-state error between the sinusoidal reference current and the output. The performance of the PR controller is highly sensitive to the grid voltage and impedance. Thus, Hamzeh et al. established a passive IDM for an inverter-based DGs where the output current at a given frequency harmonic components (e.g. 11th, 13th, or 15th) are measured [30]. The GCPVS current would resonate in the PR controller to eliminate its deviation from its reference in grid-connected mode. On the contrary, the variation of the output current is almost negligible in islanding operation due to the lack of the resonant source, i.e. the grid. The authors indicated that the functionality of the algorithm relies on the estimated admittance at PCC. In addition, the amplitude of the feedback current is defined as a trade-off between detection time and PQ degradation requirements, i.e. greater current feedback leads to a faster detection, which in turn causes a severe PQ degradation. Finally, since the algorithm may fail to detect islanding in the presence of non-linear loads, measuring the THD content of the PCC voltage has been recommended. The MATLAB/Simulink-based analyses highlighted the reliable performance of the presented IDM even in the multi-GCPVS cases, detecting islanding in less than 80 ms. The status of the PI controller in the VSI's voltage controller has been used by Das and Chattopadhyay [31]. When the GCPVS operates in parallel with the grid, the output of the PI controller remains inside the [0, 1] range, whereas it saturates during islanding. The voltage setting implemented in the GCPVS is also defined to provide low voltage ride through (LVRT). Both simulation and experimental tests highlighted the effectiveness of this IDM in at most 2 s, having the capability of seamlessly transitioning to the standalone mode. According to the proposed yardstick, this algorithm operates satisfactorily regardless of the GCPVS size and operating point without the need to set a threshold for each particular test system. However, the effect of grid disturbances such as short-circuit faults on the mentioned criterion has not been analysed. Further, the NDZ includes a large range of power imbalances, the same as those of the UVP/OVP.

Finally, some authors have exploited the voltage phase angle and its associated features, e.g. the rate of change of the voltage phase angle and its energy [32–34]. Pourbabak and Kazemi proposed the variation of the voltage phase angle as an islanding detection criterion [32], whereas Samet et al. investigated the rate of change of the phase voltage angle [33]. Both studies reported outstanding results with a reduced NDZ. In ref. [34], the rate of change of voltage phase angle, frequency, and rate of change of frequency (ROCOF) are adopted in a multifunctional technique where islanding detection, voltage support, and power sharing are addressed simultaneously.

As seen, the thresholds of the mentioned time-domain criteria in [15, 16, 23–30, 32–34] rely highly upon each particular test system. Instead, a smaller threshold mitigates the NDZ notably while the technique's maloperation in non-islanding events rises.

### 3.2.2 | Frequency-domain techniques

This type of passive-based technique take advantage of the frequency spectrum features for islanding detection purposes.

This dataset is then analysed to define a criterion in frequency-domain for classifying islanding and non-islanding events, as shown in Figure 5. In this context, the discrete wavelet transform (DWT) of PCC voltage has been developed by Balamurugan and Sahoo [35]. The islanding detection signal of this IDM is inserted into the PWM technique to de-energise GCPVS after islanding classification. The fast-islanding detection of this method (less than 20 ms) and the low voltage THD (less than 3%) have been confirmed in the presented analyses. A modified version of the continuous wavelet transform (CWT) has been exploited in ref. [36]. The identification of islanding patterns is performed by analysing a data set composed of PQ indices such as voltage amplitude, event duration time, unbalanced degree, system frequency, grid impedance, and power angle. Even though it has claimed small NDZ with no PQ degradation, it certainly injects an inter-harmonic signal whenever islanding is suspected.

In ref. [37], the instantaneous modal set of the PCC voltage has been computed, followed by a Hilbert transform. Afterwards, the variance autocorrelation of the estimated variable has been quantified. Haider et al. displayed that the variation of this criterion is negligible in grid-connected mode while it raises sharply during the islanding condition. According to the provided simulations, the presented yardstick classifies islanding with a level of accuracy greater than 97%. However, the inaccurate threshold setting may trigger GCPVS in some non-islanding events, especially induction motor starting. The standard deviation and entropy of the PCC voltage Sparse S-transform have been established by Mishra and Bhende [38]. Similar to ref. [35], a modal transform has been employed to mitigate the complexity and computational time of the presented IDM. The implemented scheme on a 14 kW GCPVS identifies islanding scenarios without false activation in non-islanding transients.

As for the time-domain techniques, tuning the appropriate threshold(s) used for islanding detection is a challenging task as in frequency-based techniques. Hence, the high dependence of these thresholds on the studied system limits the practical implementation of such schemes.

### 3.2.3 | Pattern recognition algorithms

In addition to the signal measurement/extraction of the time-domain and frequency-domain passive techniques, pattern recognition IDMs exploit a decision-making algorithm (Figure 5). In these techniques, several off-line simulations and a training process are realised based on the measured local data to classify islanding and non-islanding conditions. Machine-learning techniques such as decision tree (DT), neural network, and support vector machine (SVM) are the most extended techniques to this end. For instance, Allan and Morsi combined CWT and convolution neural network (CNN), where 31 local variables have been considered in the training process [39]. The output of the CWT is used as the initial data set required to train the CNN. Then, this technique categorises the input data into the islanding and non-islanding groups. The proposed algorithm has considered numerous case studies and exhibits 98.6% accuracy with time detection smaller than 210 ms yet its implementation is complex and costly. In addition, the number of variables and the number of samples can affect the functionality and accuracy of the IDM significantly. Gupta and Garg employed a wavelet transform on the negative-sequence of the PCC voltage [40]. Then, the extracted feature in eight frequency bands is inserted into the decision tree classifier. It is shown that the presented technique detects islanding with near-zero NDZ within 5 ms. However, the authors have carried out an extensive set of simulations to obtain the training patterns, which in turn increases the difficulty of determining the thresholds to avoid large NDZ and false tripping in non-islanding states.

Long-short term memory (LSTM) is a new robust tool for data classification [41]. The structure of LSTM is similar to the one used in a neural network but contains additional feedback connections between layers, thus being able to classify, process, and make proper predictions. Accordingly, the combination of LSTM and CWT has been recommended by Bukhari et al. in ref. [41]. Continuous wavelet transform is applied to the three-phase PCC voltage, and the amplitude and frequency of the first three bounds are inserted into the Hilbert transform to extract the instantaneous amplitude and frequency. Finally, eight features are extracted to categorise the events into the islanding and non-islanding incidents through the LSTM. The simulations endorsed the high accuracy of the presented work for both GCPVS and synchronous-based DG even in a noisy condition.

SVM is a reliable machine-learning classifier if properly assisted by a set of samples. Hence, Baghaee et al. established a new SVM-based IDM for a microgrid with GCPVS and plug-in hybrid electric vehicles (PHEVs) [42]. In this assessment, seven electrical variables are selected as features for the initial data set, including the RMS value of both current and voltage waveforms at the PCC, the THD of current and voltage signals, both active and reactive powers, and frequency. For training the SVM, a set of state variables obtained during the charging process of a PHEV are also considered as a sample. Thus, the IDM would properly identify the disturbances that occurred during this charging process as a non-islanding event. The proposed algorithm identifies the islanding condition within 40 ms with an accuracy greater than 90%. Manikonda et al. combined SVM and image classification as a reliable IDM [43]. A histogram of oriented gradient features is extracted from the image, which is used as an input feature vector for training and testing multiple SVM classifiers. Passive-based parameters such as voltage, ROCOV, and rate-of-change of negative sequence voltage are finally used to develop a strong IDM.

The pattern recognition techniques with reliable and fast detection time have drawn the attention of several researchers. However, since the settings depend largely on the system parameters, the tedious computational process required for the initial data set has to be repeated for each test system, limiting its practical application.

## 3.3 | Active-based methods

### 3.3.1 | Frequency-based techniques

The main idea of the frequency-based active IDMs is to destabilise the frequency through a periodic reactive power injection. In active frequency drift (AFD), this reactive power disturbance ($Q_{DIS}$) is injected at a given level, disregarding the size of frequency deviation [44]. The $Q_{DIS}$ is selected as a trade-off between smaller NDZ and PQ degradation, inside the following limitation:

$$Q_F\left(1-\left(\frac{f}{f_{min}}\right)^2\right) < \frac{Q_{DIS}}{P_{DG}} < Q_F\left(1-\left(\frac{f}{f_{max}}\right)^2\right) \quad (2)$$

where, $Q_F$ is the load quality factor. Further, frequency and its lower and upper standard margins are denoted by $f$, $f_{min}$, and $f_{max}$, respectively. The presented results reveal successful detection of AFD in the most stringent scenarios within 620 ms. Liu et al. developed AFD in Sandia frequency shift (SFS) technique that the $Q_{DIS}$ is injected according to the frequency deviation, i.e. a greater disturbance is employed when the frequency deviation from the nominal set is larger [45]. This reduces the NDZ and detection time of the modified technique. Further, the mentioned frequency deviation is small in non-islanding switching transients. Hence, the PQ degradation would be smaller than AFD in the grid-tied mode, 30% less current THD with the same NDZ.

### 3.3.2 | Impedance measurement

This scheme relies on measuring the equivalent impedance ($Z_{eq}$) seen by the PCC [46]. As shown in Figure 6(a), in the grid-connected mode, $Z_{eq}$ equals to the parallel of the grid's ($Z_g$) and local load's impedances ($Z_l$). This impedance would be approximately $Z_g$ which is small for a strong network. On the contrary, as illustrated in Figure 6(b), $Z_{eq}$ equals $Z_l$ being greater than $Z_g$ after the loss of mains. Therefore, a sudden rise in the impedance seen at PCC leads the system to identify islanding condition. Various methodologies attempted to integrate a disturbance in the output current at a given frequency and measure its effects on the voltage to compute $Z_{eq}$ [47–50].

The main challenge of the impedance measurement (IM) algorithm is the PQ degradation as a consequence of the injected disturbance into the current signal. Moreover, in a power plant GCPVS with several parallel GCPVSs, the inserted disturbance may imply negative voltages with opposed polarity. Thus, the total voltage and associated impedance would be influenced by such an effect, then failing to detect islanding scenarios.

The insertion of a current disturbance at high-frequencies along with IM have been presented in ref. [46]. In the presence of several DGs, Reigosa et al. suggested the deployment of the algorithm in two parallel GCPVSs to avoid the NDZ. In this master-slave approach, given GCPVS(s) is(are) responsible for islanding detection of a microgrid with several GCPVSs operating in parallel, as shown in Figure 7. This strategy is now applied in several commercial solar inverters in the range of 50–150 kW rated power, e.g. Sunny Highpower PEAK3 manufactured by SMA [51]. While the disturbance current is injected through an auxiliary circuit in ref. [46], a modified PLL has been used in ref. [47] to inject a third harmonic current disturbance. This work deploys a selective harmonic elimination (SHE) to

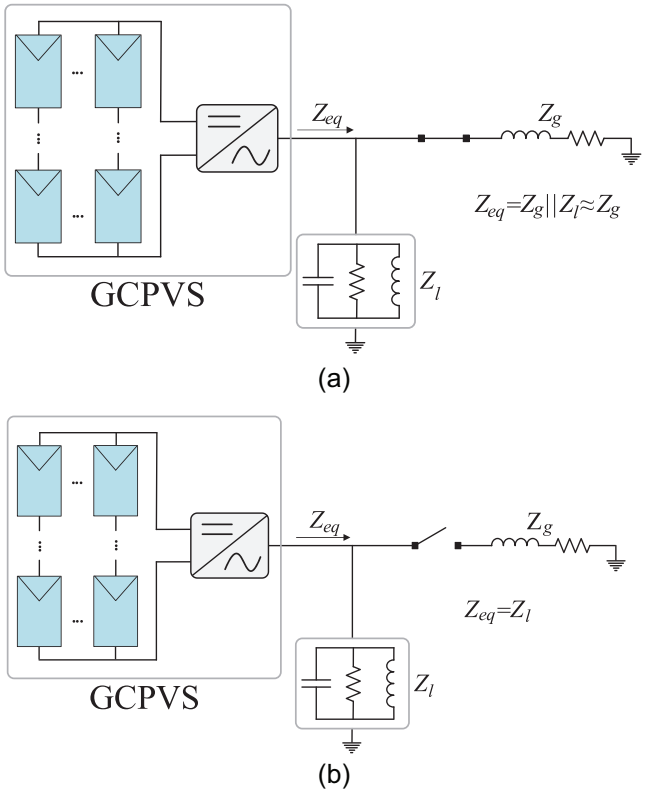


**FIGURE 6** Impedance-based measurement islanding detection scheme. (a) Grid-connected mode, (b) islanding operation

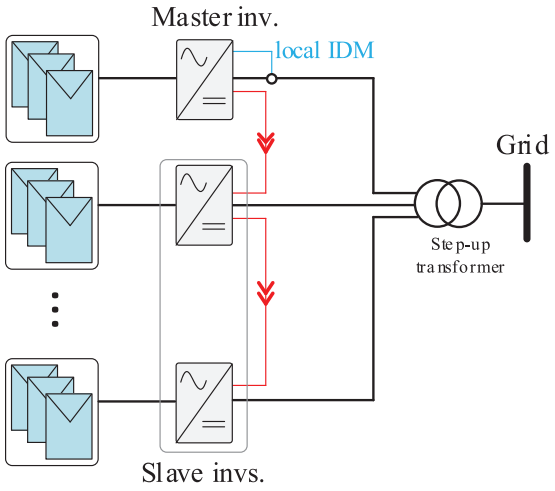


**FIGURE 7** Master–slave strategy for the effective performance of active IDMs under a multi-GCPVS scenario

remove other harmonic spectra and monitor the third harmonic current component. An improved IM-based method for single- and three-phase VSIs has been established in [48]. Reigosa et al. proposed the injection of a pulsating high-frequency signal so that the impedance of any phase in the stationary reference frame could be computed. According to the provided analysis, the presented IDM properly discriminates islanding and non-islanding events.On the other hand, the performance of the presented IDM has not been assessed under multi-DG, and high resistance short-circuits fault scenarios wherein the algorithm may operate inaccurately. While in most IM-based techniques, the disturbance current has been injected into the VSI at the PCC, Xiao et al. proposed internally triggering a short-duration short-circuit in the converter terminals to force a sharp voltage drop [49]. The short-circuit current contribution of the GCPVS to this voltage disturbance has been used for islanding detection. Despite the promising outputs, this IDM significantly deteriorates the grid PQ as occurs with other IM-based techniques.

Having said the above, it can be concluded that the aforementioned algorithms exhibit large NDZ in the presence of multi-GCPVS, cause false activation during non-islanding events when connected to a weak grid, and degrade the PQ. The aforesaid issue is of particular concern when new VSIs are connected to the nearby bus of a multi-GCPVS microgrid. The measured impedance may certainly vary as a consequence of the injected current, leading other VSIs to misclassify this event as islanding. In order to tackle this issue, Liu et al. proposed the injection of a non-fixed disturbance current and measurement of the dynamic impedance at PCC [50]. As the simulations highlighted, the recommended IDM recognises islanding operating mode with small NDZ without causing maloperation in parallel VSI starting up.

### 3.3.3 | Voltage positive feedback

In *dq0* reference frame, the GCPVS active power is commonly controlled in the VSI through *d*-axis reference current ($I_{d,\mathrm{ref}}$) while *q*-axis reference current ($I_{q,\mathrm{ref}}$) is set to zero for unity power factor operation. The destabilisation of the PCC voltage in islanding operation has been considered in the positive voltage feedback (VPF). In this IDM, a feedback of the PCC voltage has been inserted into the $I_{d,\mathrm{ref}}$ as follows [52]:

$$I_{d,\mathrm{ref}} = (P_{\mathrm{ref}} - P_{\mathrm{DG}})\left(k_{\mathrm{P}} + \frac{k_{\mathrm{I}}}{s}\right) + (k_{\mathrm{PF}} \times \Delta V_{\mathrm{PCC}}) \quad (3)$$

where, $P_{\mathrm{ref}}$ is the active power reference. Moreover, positive feedback gain ($k_{\mathrm{PF}}$) controls the size of injected disturbance. Based on Eq. (3), $I_{d,\mathrm{ref}}$ increases during an islanding operation under $\Delta V_{\mathrm{PCC}}>0$ with a surplus of active power (see Equation (1)). Therefore, $P_{\mathrm{DG}}$ reaches a greater setpoint leading to a further PCC voltage rise. This procedure continues until $V_{\mathrm{PCC}}$ exceeds the standard upper limit and OVP de-energises GCPVS. For islanding scenarios with $\Delta V_{\mathrm{PCC}}<0$, $I_{d,\mathrm{ref}}$ reduces $P_{\mathrm{DG}}$ continuously so that $V_{\mathrm{PCC}}$ goes beyond the minimum standard

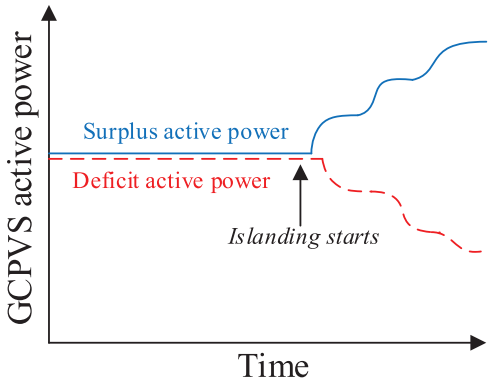


**FIGURE 8** Voltage positive feedback performance in islanding events

set as illustrated in Figure 8. The upper and lower bounds of $k_{\mathrm{PF}}$ are defined to achieve the minimum NDZ and maximum stable performance of the GCPVS during non-islanding disturbances, respectively. Samui and Samantaray underscored the reliable performance of the VPF in the presence of constant impedance, current, and power loads with a detection time of 1 s [53]. It was also shown in ref. [54] that even though VPF changes the current amplitude, it does not imply an increase in the harmonic/subharmonic content, which assures reduced PQ degradation.

The primary source of GCPVS in refs. [52, 53] has been modelled as a DC voltage source. This source acts as an infinite power source and feeds any DC current in a given constant DC voltage. It is worth pointing out that in these studies, the input power of the GCPVS is limited in any operating condition by modelling the PV array and its MPPT algorithm. Therefore, the conventional VPF fails to raise $P_{\mathrm{DG}}$ during surplus active power scenarios and suffers from an NDZ within the range [0%, 17.35%]. Thus, the injection of the absolute voltage negative feedback (VNF) has been proposed as follows to overcome this issue [55]:

$$I_{d,\mathrm{ref}} = (P_{\mathrm{ref}} - P_{\mathrm{DG}})\left(k_{\mathrm{P}} + \frac{k_{\mathrm{I}}}{s}\right) - |k_{\mathrm{NF}} \times \Delta V_{\mathrm{PCC}}| \quad (4)$$

Similarly to the VPF, the amplitude of the imposed disturbance ($k_{\mathrm{NF}}$) has been defined to ensure minimum NDZ and large stable operation during non-islanding transients. This disturbance injection ensures that the PCC voltage is pushed down to the lower bound in all possible scenarios. Consequently, the enhanced algorithm fixes the input power limitation and can be implemented regardless of the PV operation point. The simulation results under numerous case tests highlighted that the VNF technique identifies all islanding conditions in less than 810 ms.

### 3.3.4 | Other active algorithms

The idea of inserting an intentional disturbance into the GCPVS and observing its effects on the system variables (in either voltage or frequency) has been reported by some researchers [56,

57]. For instance, Sivadas and Vasudevan slightly modified the $P_{DG}$ around the rated point of operation and measured the *d*-axis equivalent resistance at PCC [56]. It's been shown that the mentioned yardstick tracks the $P_{DG}$ fluctuations during grid-connected mode, whereas it remains almost fixed in islanding operation. The presented equations in two parallel GCPVSs implied the necessity of the same $P_{DG}$ change by applying a global positioning system (GPS) to avoid misclassification. Further, these equations for a system with more than two units are eminently complex. This technique has been evaluated in an experimental test and detects the islanding condition with zero active power imbalance within 500 ms. In addition to the costly implementation, this IDM is also heavily sensitive to the simultaneous disturbance injection in a multi-GCPVS case as it has been reported for IM-based IDMs.

## 3.4 | Hybrid methods

In hybrid techniques, the process of injecting an active disturbance is initiated whenever the islanding operation is suspected through a passive criterion. The combination of both active- and passive-based methods significantly reduces the overall NDZ compared to the pure passive IDM without violating the PQ standards in grid-connected mode. As an instance of hybrid schemes, the active power output of GCPVS has been reduced through a current injection into $I_{d,\text{ref}}$ during suspicious islanding events, categorised by an absolute voltage deviation index [58]. This power curtailment leads to a further voltage reduction; thus, islanding is recognised when voltage and active power output drop below pre-defined thresholds simultaneously. The thresholds of the second level have been defined irrespective of the GCPVS size and control loop; however, the voltage threshold in the first stage has been determined as a trade-off between small NDZ and false tripping of non-islanding events. Since islanding is detected in less than 300 ms without shifting voltage beyond the standards, the GCPVS would remain stable after islanding detection, facilitating the smooth transition between grid-connected and islanded microgrid. The combination of four active and three passive IDMs has been developed by Barkat et al. [59]. This IDM identifies numerous islanding scenarios in a single-phase GCPVS system within 148 ms without any false tripping during non-islanding cases. Implementing these algorithms is costly, especially for single-phase VSIs commonly smaller than 5 kW and used for residential GCPVSs.

Some researchers have proposed the connection of several types of impedances in a two-stage process [60, 61]. This additional load is connected in the case that the passive criterion of the first stage is exceeded. This load connection forces the state variables to exceed the passive-based criterion in the second stage during islanding incidents without significant effect on the non-islanding transients. Rostami et al. have demonstrated that the connection of a reactance would discriminate islanding events effectively [60]. The fast Fourier transform is initially applied to the PCC voltage to compute ROCOV. According to the estimated ROCOV, the non-islanding (ROCOV≤250%/s) and suspicious events (ROCOV>250%/s) are categorised. The

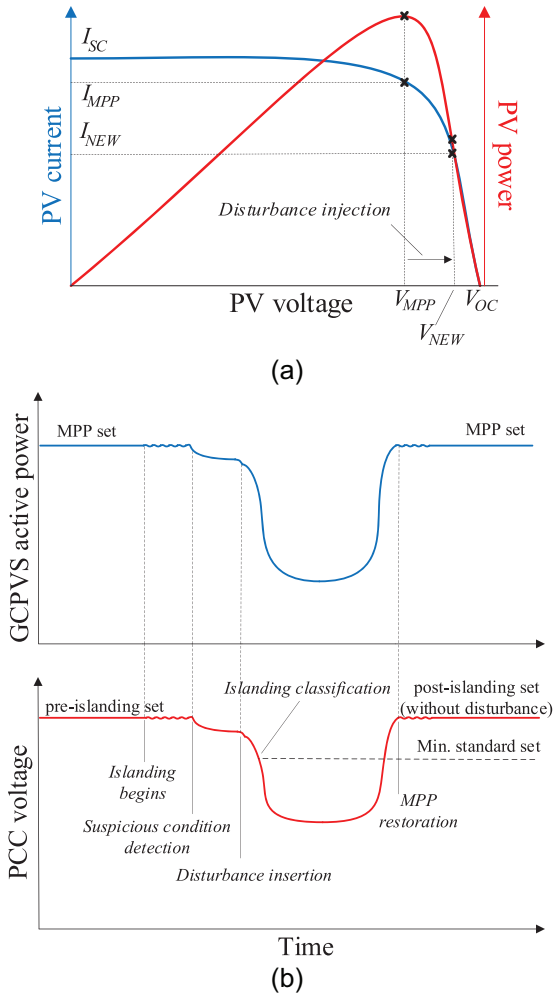


**FIGURE 9** MPPT-based islanding detection technique. (a) Power reduction due to MPP loss, (b) PCC voltage drop

reactance is then connected to the PCC throughout suspicious events, leading to ROCOV values greater than 10%/s. Although this IDM identifies most islanding scenarios within 300 ms, the mentioned thresholds have been defined by simulations and may have to be substantially redefined if a new system is to be considered. In ref. [61], a resistance-capacitance parallel load has been switched ON if measured ROCOF and ROCOV settings are exceeded ($2 \times 10^{-3}$ Hz/s and $2 \times 10^{-3}$ pu/s) considering minimum voltage supervision of 85%. Based on the achieved results, islanding is detected even with negligible active and reactive power mismatches in the order of $2 \times 10^{-3}$%. Moreover, this study has considered the frequency deviations as non-islanding events for the first time.

The MPPT algorithm extracts the maximum available power of the PV array in any given operating condition. Based on this, a two-level IDM has been presented for GCPVS to slightly shift the MPP whenever islanding is suspected [62]. This MPP curtailment leads to an active power output reduction which triggers the islanding detection signal, as shown in Figure 9. In this figure, the voltage and current associated with the MPP and post-disturbance injection are denoted by "MPP" and "NEW" subscripts, respectively. Moreover, $I_{SC}$ and $V_{OC}$

stand for short-circuit current and open-circuit voltage of the PV array, respectively. In ref. [63], suspicious events are firstly defined by absolute voltage deviation, followed by a disturbance injection into the PV array voltage. The size of the disturbance voltage is defined so that the active power output shifts the PCC voltage from the upper standard set (110%) to the lower edge (88%) as the worst case. The mentioned disturbance is cleared after a given time delay; so the GCPVS restores the MPP to switch the GCPVS between grid-connected to a standalone operation whilst delivering the maximum available active power. This IDM has been improved by injecting a disturbance into the DC/DC duty cycle in ref. [63]. Crucially, the thresholds do not depend on the PV array characteristics. It also identifies islanding without causing any significant voltage drop, facilitating the PCC voltage recovery. Both IDMs show accurate and fast performance even in the challenging scenarios with negligible power imbalances, i.e. the NDZ is [−2%, +2%] and [−1%, +1%] of $\Delta P/P_{\mathrm{DG}}$ for refs. [62] and [63], respectively. Moreover, these IDMs have no false operation in non-islanding disturbances and short-circuit faults as they are structured to avoid simultaneous voltage and power drops in such cases.

In ref. [64], after the injection of a 1% disturbance current at the frequency of 20 Hz, the *d*-axis component of the PCC voltage ($V_d$) is analysed. It was shown that the deviation of this component from its reference signal in grid-connected mode ($V_{d,\mathrm{ref}}$) and its derivative feature efficiently and effectively detect the islanding operation. The extensive test cases remarked that this IDM classifies islanding under various power imbalances, load quality factors, and multi-GCPVS scenarios within 130 ms. Finally, the authors demonstrated the reliable performance of the adaptive $V_{d,\mathrm{ref}}$ setting under all operating points, e.g. received solar irradiations for GCPVS.

## 4 | COMPARISON OF EXISTING ALGORITHMS

This section presents an in-depth comparison of the presented IDMs for GCPVS. In this comparison, the main considered features are the NDZ, detection time, applicability in an autonomous microgrid, PQ degradation, and the level of cost and complexity.

### 4.1 | Non-detection zone

Non-detection zone is a clear indicator of the reliability of an IDM as it shows the expected undetected region. This zone is defined by both active and reactive power mismatches wherein the employed IDM fails to identify the islanding condition within 2 s. The NDZ is defined through the outputs of the IDM assessment in the cases defined in the IEEE Std. 1547-2018 [7] and UL 1741 [8]. Further, the presented IDMs should not exhibit maloperation in non-islanding switching transients. The effectiveness of the existing IDMs for GCPVS in islanding and non-islanding test cases are summarised in Table 1, categorised into zero/small, medium, and large.

It is evident that the remote IDMs are reliable classifiers in all possible islanding and non-islanding events. These schemes are a dependable solution for all microgrids if a fast broadband telecommunication infrastructure is available. As mentioned earlier, the NDZ of the most passive IDMs has been reduced slightly and yet still some of them exhibit undetectable regions. Since the grid controls the local variables in non-islanding disturbances, the false tripping of such IDMs in these switching transients is small. Active and hybrid IDMs have shown a similar performance as the one achieved in passive-based techniques. The recent algorithms classify islanding and non-islanding events with high accuracy, except VPF with a large NDZ. Moreover, a few active techniques such as IM and *d*-axis equivalent resistance misclassify islanding in multi-GCPVS cases.

### 4.2 | Detection time

In a distribution network, most reclosures are set to operate at 0.1–0.3s as the fast reclosing, trying to restore the islanded microgrid after the occurrence of transient faults [65]. If the islanding protection does not activate before this reclosing, an out-of-phase reconnection can occur implying undesired transient over voltages with at most 2 pu. This over voltage may damage the loads, the equipment of the GCPVS, and the step-up transformer. Hence, fast islanding protection mitigates the chance of unsynchronised reclosing and its adverse effects under such protection scheme. Further, the recently released IEEE Std. 1547-2018 suggests keeping the GCPVS operating in the standalone microgrid after islanding has been detected [7]. Although the abovementioned standard and UL 1741 are aligned with the system operators protocols where it is advised to identify the islanding condition on within 2 s [7, 8], a fast performance allows the system to fulfil such requirements whilst ensuring a smooth transition to the autonomous mode. In this vein, the detection time has been measured and reported in the literature as depicted in Figure 10. Since the performance of the remote schemes depends on the type of telecommunication channeland the implemented protocol, it can noticeably affect the detection time, these IDMs are excluded in this figure. Based on these data, most frequency-based and pattern recognition IDMs identify islanding events in less than 200 ms. Nevertheless, the vast majority of the active and hybrid methodologies require larger time frames to shift a local criterion outside of the pre-set limits through the disturbance. The detection time of such IDMs falls mainly within the time range [0.2 s, 1 s].

According to Figure 10, it can be generally concluded that most pattern recognition-based IDMs identify the islanding operation within an acceptable detection time, i.e. most of them in less than 1 s.

### 4.3 | Applicable for standalone microgrid

As mentioned in the last subsection, standards and system operators have emphasised the importance of providing

**TABLE 1** NDZ of islanding detection techniques for GCPVSs

| Methodology | NDZ | | | Maloperation in non-islanding events |
|---|---|---|---|---|
| | Zero/small | Medium | Large | |
| Remote | DTT [9]<br>Power line signalling [10, 11]<br>Distributed communication-based [12] | – | – | Zero |
| Passive-based (Time-domain) | Transient voltage function [23]<br>Maxima of superimposed voltage components [25]<br>CRPH [26]<br>Piecewise $P_{DG}$ vs. $V_{PCC}$ function [27]<br>ROCOV and VoI [28]<br>PR controller feedback [30] | PCC voltage ripple [24]<br>ROCOP and ROCOV [29] | UVP/OVP [15]<br>PI controller saturation [31] | Several cases |
| Passive-based (Frequency-domain) | DWT [35]<br>Autocorrelation of PCC voltage modal envelop [37] | – | – | Few cases |
| Passive-based (Pattern recognition) | S-transform of PCC voltage [38]<br>CWT and CNN [39]<br>CWT and DT [40]<br>SVM [42] | – | – | Few cases |
| Active-based | IM [46–50]<br>Absolute VNF [54]<br>*d*-axis equivalent resistance [56] | AFD [44]<br>SFS [45] | VPF [52–54] | Few cases |
| Hybrid | Absolute voltage deviation and disturbance injection into $I_{d,ref}$ [58]<br>Combination of passive and active methods [59]<br>Impedance switching [60, 61]<br>MPPT disturbance injection [62]<br>DC/DC converter's duty cycle disturbance injection [63]<br>*d*-axis current injection with PCC voltage supervision [64] | – | – | Few cases |

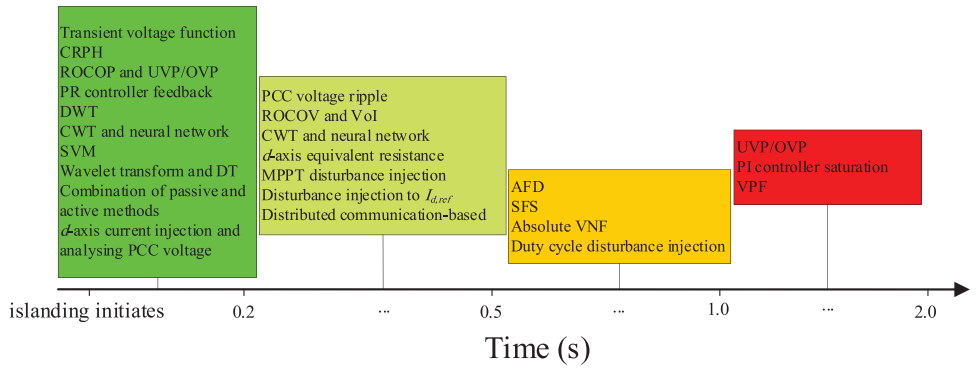


**FIGURE 10** Detection time of islanding detection methodologies for GCVPSs

a continuous power supply to the critical loads in the microgrid. Besides fast islanding detection, the frequency and voltage recovery should be conducted to shift smoothly the DGs to the autonomous mode. From this perspective, the employed IDM should cause a sufficient frequency/voltage deviation to identify islanding without destabilizing the GCPVS; thus, it provides both islanding detection and facilitates a seamless transition to standalone mode. Since passive and remote schemes do not inject a disturbance, this part focuses on active and hybrid methodologies.

Most active techniques have been designed to shift a local variable by injecting a periodic disturbance [44–50, 51–57].

**TABLE 2** Effect of PQ degradation in active and hybrid IDMs

| Methodology | PQ degradation |
|---|---|
| Active frequency drift [44] | Large |
| Sandia frequency shift [45] | Medium |
| Impedance measurement [46–50] | Small |
| Voltage positive feedback [52–54] | Small |
| Absolute voltage negative feedback [55] | Small |
| *d*-axis equivalent resistance [56] | Small |
| Impedance switching [60, 61] | Small |
| MPPT disturbance injection [62] | Small |
| DC/DC converter's duty cycle disturbance injection [63] | Small |

**TABLE 3** Cost and complexity of GCPVS-based IDMs

| Methodology | Threshold dependency; tuning process | Cost and complexity |
|---|---|---|
| Remote | – | Large |
| Time-domain passive | Mostly high; some analytically | Small |
| Frequency-domain passive | High; mostly through simulation/experimental tests | Medium |
| Pattern recognition | Too high; through simulation/experimental tests | Large |
| Active | Mostly high; some analytically | Medium |
| Hybrid | Mostly high; some analytically | Medium |

Therefore, the GCPVS would be destabilised after islanding detection, and its restoration would be infeasible. The transition between grid-connected and autonomous mode would also be time-consuming for a few hybrid IDMs as they attempt to drive a local variable outside the standard range in suspicious islanding events. For example, the MPPT disturbance injection forces the PCC voltage beyond the minimum standard set [62]. Still, most hybrid techniques are designed to slightly change the system conditions of the microgrid/GCPVS for islanding detection without destabilizing the islanded area [58–61, 63, 64]. For example, a slight active power output reduction is ordered in refs. [58] and [63] to cause a $V_{PCC}$ drop for identifying the islanding operation yet meeting the voltage grid requirements. Therefore, keeping the PCC voltage within the standard range guarantees a smooth voltage recovery for a successful transition to standalone mode.

## 4.4 | Power quality degradation

As mentioned above, the main pillar of both active and some hybrid IDMs lies in the injection of a disturbance to the VSI, which in turn undermines the PQ of the grid. In AFD and SFS, the harmonic current is injected to drift frequency out of the established IDM thresholds. This disturbance current has been limited to a given setpoint to meet the PQ standard requirements. A harmonic current is used in the IM to detect islanding through the measured harmonic voltage. In this scheme, islanding can be identified taking advantage of a smaller harmonic current than AFD and SFS. This concern has been fixed in the recent voltage-based active and hybrid IDMs, as presented in Table 2. In these techniques, rather than harnessing frequency or current angle, the current amplitude of the fundamental frequency would be modified for islanding detection purposes. For instance, it is revealed that for a given 1 kW GCPVS, the THD and harmonic spectra of the output current in VPF and modified sliding mode controller meets the IEEE Std. 1547–2018 requirements [7] for a wide range of disturbance sizes and operating points [54].

## 4.5 | Level of cost and complexity for realisation

Several IDMs have been reported with small NDZ and detection time. Nonetheless, an inexpensive structure and a low computational time process for thresholds determination are required for practical implementation. These features have been considered in this section.

As elaborated earlier and presented in Table 3, the main shortage of the remote schemes is the expensive telecommunication infrastructure. On the contrary, most local IDMs can be realised simply and cost-effectively. However, the existing challenge of most IDMs is the thresholds dependency on the studied GCPVS/grid characteristics. Furthermore, these thresholds have been defined after performing numerous islanding and non-islanding simulations/experimental tests without supporting evidence of the employed analytical expressions. Therefore, these tests should be repeated for a new GCPVS/grid. The structure of the time-domain passive IDMs and active techniques is simple, whereas the majority of frequency-based and pattern recognition algorithms suffer from complex realisation. These passive IDMs need a complex signal processing technique for feature extraction/decision making. As the hybrid IDMs use both active and passive methods, the implementation of such schemes may also be complex and expensive.

# 5 | REVIEW OF ADVANCED FUNCTIONALITIES IN ISLANDING DETECTION STUDIES

This section aims to review the state-of-the-art of the current requirements and advanced functionalities for GCPVS in grid-following mode according to the grid codes and standards. Indeed, as these services have become mandatory for new products, the interaction between islanding detection and these capabilities still needs to be explored at great length. In this regard, the recently published works considering simultaneous IDM and other functions are detailed.

The DGs are expected to support ancillary services for boosting grid reliability as emphasised in the recently published grid codes [66, 67]. Even though the grid codes may vary according to each country and operator, there is a general agreement on the role that GCPVSs must play when connected to the grid. In this context, outstanding work has been carried out by Demoulias et al. [68] which extensively recalls the features of the ancillary services and unveils their prospects. The recently added technical requirements for GCPVS can be summarised as follows;

- LVRT (also known as fault-ride-through)
- Reactive power control and voltage support
- Active power and frequency support
- Inertia emulation

The LVRT is the capability of a generation unit to withstand a voltage sag whilst providing reactive power due to a fault in the electrical grid. Thus, the GCPVS is expected to inject reactive power according to a given curve during these events to mitigate the effects of this fault [68, 69]. Even though the grid codes only stand for the reactive power and duration, the need to unfold such schemes given the resistance to reactance ratio of the grid has been stressed in ref. [70]. To the best of our knowledge, only two works have so far explored the simultaneous implementation of LVRT and IDM [31, 71].

The established procedures for voltage regulation in DNs have been studied and debated between scientists and electrical engineers for some time now. But still, the presence of the GCPVSs units has undeniably made such a goal more challenging given their inherent intermittency [72]. Thus far, the latest research has suggested multi-agent cooperative action to effectively fulfil voltage control [73]. Therefore, the GCPVS will sooner or later be a vital asset for voltage control as it can regulate its reactive power contribution. Against this backdrop, the IDMs must be appropriately coordinated to meet these voltage/reactive power requirements and avoid undesired maloperation in grid-connected mode. The effects of simultaneous implementation of voltage support with IDM have been scrutinised in ref. [34]. The obtained results readily indicate that the system can accomplish these two functions simultaneously, given any power mismatch or operating condition. Further research could focus on testing the islanding capability in scenarios with multiple GCPVSs where all units are engaged in a joint reactive scheme.

The active power-frequency control lies in keeping the balance between generation and demand, and such responsibility falls typically within the transmission and/or system operator who establishes the protocols [74]. Hence, the GCPVS is expected to remain connected and contribute to restoring the system frequency by increasing the output power. For instance, when this parameter drops below a certain threshold due to a mismatch between generation and load. The surplus of active power supplied by the GCPVS is determined according to the size of the unit and severity of the event, i.e. the $P_{DG}$–$f$ curve included in the grid codes [75]. Up to this point, it can be seen to which extent the above criterion must be scrupulously followed to avoid further generation curtailment, which could aggravate the problem even more [76]. It is worth noting that the grid-tied PV units involved in an active power/frequency unit commitment could face a conflict between the two functions as one can order tripping, whereas the other could suggest the opposite. Based on the above, the simultaneous implementation of IDM and frequency support would be of particular interest for future research as GCPVS has to meet the $P_{DG}$–$f$ requirements while identifying an island at distribution levels.

The latest functionality under scrutiny is the so-called inertia emulation. Conceptually, this feature has been specifically designed for the converter-based generators to act as synchronous ones [77]. Thence, these units can play a part in restoring the inertia reduction after removing synchronous generators. These virtual DGs were initially implemented in large power plants connected to transmission networks [78]. However, the recently mentioned codes state that even DG with a small size will be required to incorporate such features. Recently, the islanding detection capability has been studied, for the first time, in a virtual synchronous generator by Shi et al. [79].

In addition to the previously mentioned technical requirements covered by the grid codes, other approaches could also be very useful for the grid operator, e.g. a PMU-based IDM considering cyber-attacks in ref. [80].

In the authors' view, the GCPVSs can also be considered a reliable asset to address the unbalances caused by the large penetration of single-phase GCPVS or as main sources in intentional islanding operations targeted at reducing power interruptions in DNs. Therefore, future lines of research will be focused on addressing several functionalities in combination with the islanding detection to surmount the upcoming challenges.

## 6 | CONCLUSIONS AND RECOMMENDATIONS FOR FUTURE IMPROVEMENTS

This paper reviews the recent islanding detection developments for GCPVSs. The existing algorithms and the corresponding highlights are initially recalled and then compared thoroughly. According to the existing IDMs, it is found that:

- Application of remote schemes with secure performance is growing due to the development of the communication infrastructure, e.g. 5G and fast fibre optic. Nevertheless, the high burden cost is still the main limitation of such IDMs for small-scale residential GCPVS applications for instance.
- The NDZ has been eminently reduced in the recently developed passive IDMs, especially those that use pattern recognition algorithms. The main challenge of such IDMs is determining the thresholds as they depend highly on the test system under study and GCPVS characteristics.
- The negative effects in the output PQ have been alleviated in the recent active IDMs by adapting the current amplitude of the fundamental frequency instead of injecting a current signal with either harmonic or subharmonic content. That said, the destabilisation caused by this injected signal in the

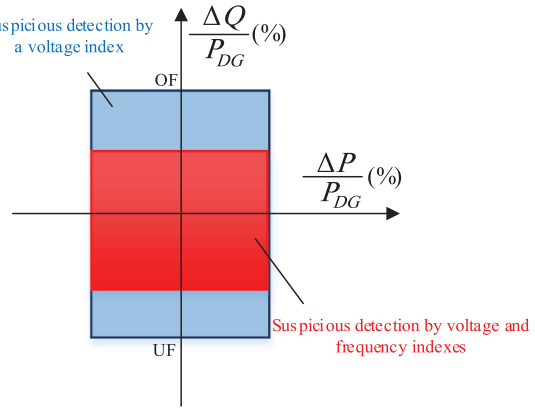


**FIGURE 11** Non-detection zone reduction of hybrid IDMs by identifying suspicious events through voltage and frequency indices

GCPVS impedes fulfilling a seamless transition to standalone mode after the islanding condition.

- The hybrid schemes have effectively mitigated the PQ degradation and NDZ. However, the complex structure and large detection time, e.g. up to 1 s in most cases, are the main demerits of these IDMs.
- Recent studies have proposed simultaneous LVRT and IDM [31, 70] but do not consider cases with a negligible power imbalance. Other approaches have analysed the performance of a microgrid with both a GCPVS and energy storage systems to provide voltage support, islanding detection, and load sharing but missed to consider ancillary services [34].
- It is seen that some schemes proved to be very effective for IDM, accomplishing a reduced NDZ and robustness during the non-islanding events. Nevertheless, non-islanding disturbance events caused by large-scale generation-load imbalances have not been considered. Indeed, a massive GCPVS tripping during these events would even aggravate the situation, leading to higher frequency instability [74].

Based on the analysis provided in Sections 5 and 6, the following insights can be drawn to improve the existing techniques while meeting the grid codes:

- As the penetration of RESs such as GCPVS in electric power systems has been increased, they would be required to provide ancillary services. Therefore, the interaction between these features and islanding detection should draw more attention in future studies.
- Several hybrid methodologies employed a voltage-based criterion to identify the suspicious islanding events [58, 62–64]. The NDZ of such IDMs in the horizontal axis ($\Delta P/P_{DG}$) can be mitigated by selecting a smaller threshold without significantly affecting the vertical axis ($\Delta Q/P_{DG}$). To overcome such shortcomings, the frequency criterion can be added to complement the voltage threshold, developing a multi-criteria islanding detection approach also covering events with reactive power imbalance (Figure 11).
- As stated above, some methodologies employing frequency and/or ROCOF as main variables for IDM [44-50] or as a part of the algorithm thereof, i.e. pattern recognition techniques [41-43], will need to be reassessed considering non-islanding frequency events as those displayed in ref. [].

In order to meet the IEEE Std. 1547-2018 and UL 1741 requirements such as zero NDZ and acceptable PQ, most VSI manufacturers combine two or more techniques; e.g. AFD and ROCOF [51, 81, 82]. In such techniques, each IDM covers the shortages of the other algorithm. Therefore, the combination of the passive and active IDMs can be considered by researchers for future trends.

Finally, it is worth saying that valuable islanding detection reviews have been published recently [3–5]. However, by observing the discussion provided in Sections 4–6, the novelty of the present review when compared with the previous ones is underscored. These two reviews focused on gathering the previously published ID methods and classifying them according to the different sub-types. On the contrary, our approach not only has considered an updated survey of the previously published IDMs so far but broadened the scope of these studies by bringing up their future trends.

## CONFLICTS OF INTEREST

The authors declare no conflict of interest.

## DATA AVAILABILITY STATEMENT

The authors hereby confirm the availability of provided data (analyses, discussions etc.) in this paper.

## ORCID

*Reza Bakhshi-Jafarabadi* https://orcid.org/0000-0001-5362-304X
*Javad Sadeh* https://orcid.org/0000-0002-3331-2508
*Alexandre Serrano-Fontova* https://orcid.org/0000-0002-5147-6055

## REFERENCES

1. Jäger-Waldau, A.: Snapshot of photovoltaics—February 2020. Energies 13(4), 1–8 (2020)
2. Uzum, B., Onen, A., Hasanien, H.M., Muyeen, S.M.: Rooftop solar PV penetration impacts on distribution network and further growth factors—a comprehensive review. Electron 10(1), 1–31 (2020)
3. Worku, M.Y., Hassan, M.A., Maraaba, L.S., Abido, M.A.: Islanding detection methods for microgrids: a comprehensive review. Mathematics 9(24), 1–23 (2021)
4. Mishra, M., Chandak, S., Rout, P.K.: Taxonomy of islanding detection techniques for distributed generation in microgrid. Renewable Energy Focus 31, 9–30 (2019)
5. Panigrahi, B.K., Bhuyan, A., Shukla, J., Ray, P.K., Pati, S.: A comprehensive review on intelligent islanding detection techniques for renewable energy integrated power system. Int. J. of Energy Research 45(10), 14085–14116 (2021)
6. Serrano-Fontova, A., Torrens, P.C, Bosch, R.: Power quality disturbances assessment during unintentional islanding scenarios. A contribution to voltage sag studies. Energies 12(16), 1–21 (2019)
7. IEEE Standard 1547-2018: IEEE Standard for interconnection and interoperability of distributed energy resources with associated electric power systems interfaces (2018). Accessed 15 February 2018
8. UL standard 1741 revision: Standard for inverters, converters, controllers and interconnection system equipment for use with distributed energy resources (2016). Accessed 7 September 2016

9. Dob, B., Palmer, C.: Communications assisted islanding detection: contrasting direct transfer trip and phase comparison methods. In: 2018 71st Annual Conference for Protective Relay Engineers (CPRE). pp. 1–6. IEEE, Piscataway, NJ (2018)
10. Cataliotti, A., Cosentino, V., Di Cara, D., Guaiana, S., Panzavecchia, N., Tine, G.: A new solution for low-voltage distributed generation interface protection system. IEEE Trans. Instrum. Meas. 64(8) 2086–2095 (2015)
11. Bayrak, G., A remote islanding detection and control strategy for photovoltaic-based distributed generation systems. Energy Convers. Manage. 96, 228–241 (2015)
12. Ma, J. et al.: An islanding detection and prevention method based on path query of distribution network topology graph. IEEE Trans. Sustainable Energy 13(1), 81–90 (2022)
13. Song, W., Chen, Y., Wen, A., Zhang, Y., Wei, C.: Detection and switching control scheme of unintentional islanding for hand in hand DC distribution network. IET Gener. Transmiss. Distrib. 13(8), 1414–1422 (2019)
14. Firmware manual PVS800-57B central inverters. www.library.e.abb.com/public/e3265ca64c964373c1257b94002ba867/FR_PVS800_FW_A_with%20update%20notice_12_2011.pdf (2022). Accessed 1 March 2022
15. Yingram, M., Premrudeepreechacharn, S.: Investigation over/under-voltage protection of passive islanding detection method of distributed generations in electrical distribution systems. In: 2012 International Conference on Renewable Energy Research and Applications (ICRERA), pp. 1–5. IEEE, Piscataway, NJ (2012)
16. Hassan, A.A.M., Kandeel, T.A.: Effectiveness of frequency relays on networks with multiple distributed generation. J. Elect. Syst. and Inf. Technol. 2(1), 75–85 (2015)
17. Do, H.T., Zhang, X., Nguyen, N.V., Li, S., Chu, T.T.-T.: Passive islanding detection method using wavelet packet transform in grid connected photovoltaic systems. IEEE Trans. Power Electron. 31(10), 6955–6967 (2016)
18. Cui, Q., El-Arroudi, K., Joos, G.: Islanding detection of hybrid distributed generation under reduced non-detection zone. IEEE Trans. Smart Grid 9(5), 5027–5037 (2018)
19. Bakhshi, R., Sadeh, J.: Voltage positive feedback based active method for islanding detection of photovoltaic system with string inverter using sliding mode controller. Sol. Energy 137, 564–577 (2016)
20. Seyedi, M., Taher, S.A., Ganji, B., Guerrero, J.M.: A hybrid islanding detection technique for inverter-based distributed generator units. Int. J. Elect. Power Energy Syst. 29(11), 1–21 (2019)
21. Ali Khan, M.Y., Liu, H., Yang, Z., Yuan, X.: A comprehensive review on grid connected photovoltaic inverters, their modulation techniques, and control strategies. Energies 13(16), 1–40 (2020)
22. Bollipo, R.B., Mikkili, S., Bonthagorla, P.K.: Critical review on PV MPPT techniques: classical, intelligent and optimisation. IET Renewable Power Gener. 14(9), 1433–1452 (2020)
23. Dubey, R., Popov, M., Samantaray, S.R.: Transient monitoring function-based islanding detection in power distribution network. IET Gener. Transm. Distrib. 13(6), 805–813 (2018)
24. Guha, B., Haddad, R.J., Kalaani, Y.: Voltage ripple-based passive islanding detection technique for grid-connected photovoltaic inverters. IEEE Power Energy Technol. Syst. J. 3(4), 143–154 (2016)
25. Kumar, P., Kumar, V., Pratap, R.: FPGA implementation of an islanding detection technique for microgrid using periodic maxima of superimposed voltage components. IET Gener. Transm. Distrib. 14(9), 1673–1683 (2020)
26. Haider, R., Ghanbari, T., Kim, C.-H.: Islanding detection scheme for inverter-based distributed generation systems using cumulative reactive power harmonics. J. Elec. Eng. Technol. 14(5), 1907–1917 (2019)
27. Kamyab, E., Sadeh, J.: Islanding detection method for photovoltaic distributed generation based on voltage drifting. IET Gener. Transmiss. Distrib. 7(6), 584–592 (2013)
28. Karimi, M., Farshad, M., Hong, Q., Laaksonen, H., Kauhaniemi, K.: An islanding detection technique for inverter-based distributed generation in microgrids. Energies 14(1), 1–18 (2020)
29. Elshrief, Y.A., Helmi, D.H., Abd-Elhaleem, S., Abozalam, B.A., Asham, A.D.: Fast and accurate islanding detection technique for microgrid connected to photovoltaic system. J. Radiat. Res. Appl. Sci. 14(1), 210–221 (2021)
30. Hamzeh, M., Rashidirad, N., Sheshyekani, K., Afjei, E.: A new islanding detection scheme for multiple inverter-based DG systems. IEEE Trans. Energy Convers. 31(3), 1002–1011 (2016)
31. Das, P.P., Chattopadhyay, S.: A voltage-independent islanding detection method and low-voltage ride through of a two-stage PV inverter. IEEE Trans. Ind. Appl. 54(3), 2773–2783 (2018)
32. Pourbabak, H., Kazemi, A.: Islanding detection method based on a new approach to voltage phase angle of constant power inverters. IET Gener., Transm. Distrib. 10(5), 1190–1198 (2016)
33. Samet, H., Hashemi, F., Ghanbari, T.: Islanding detection method for inverter-based distributed generation with negligible non-detection zone using energy of rate of change of voltage phase angle. IET Gener., Transm. Distrib. 9(15), 2337–2350 (2015)
34. Serrano-Fontova, A., Azab, M.: Development and performance analysis of a multi-functional algorithm for AC microgrids: simultaneous power sharing, voltage support and islanding detection. Int. J. Elect. Power Energy Syst. 135, 107341 (2022)
35. Balamurugan, M., Sahoo, S.K.: A novel islanding detection technique for grid connected photovoltaic system. Appl. Solar Energy 53(3), 208–214 (2017)
36. Paiva, S.C., de Araujo Ribeiro, R.L., Alves, D.K., Costa, F.B., de Oliveira Alves Rocha, T., A wavelet-based hybrid islanding detection system applied for distributed generators interconnected to AC microgrids. Int. J. Elect. Power Energy Syst. 121, 1–10 (2020)
37. Haider, R. et al.: Passive islanding detection scheme based on autocorrelation function of modal current envelope for photovoltaic units. IET Gener., Transm. Distrib. 12(3), 726–736 (2017)
38. Mishra, P.P., Bhende, C.N.: Islanding detection using sparse S-transform in distributed generation systems. Elect. Eng. 100(4), 2397–2406 (2018)
39. Allan, O.A.,Morsi, W.G.: A new passive islanding detection approach using wavelets and deep learning for grid-connected photovoltaic systems. Electric Power Syst. Research 199, 1–11 (2021)
40. Gupta, N., Garg, R.: Algorithm for islanding detection in photovoltaic generator network connected to low-voltage grid. IET Gener. Transmiss. Distrib. 12(10), 2280–2287 (2018)
41. Bukhari, S.B.A., Mehmood, K.K., Wadood, A., Park, H.: Intelligent islanding detection of microgrids using long short-term memory networks. Energies 14(18), 1–16 (2021)
42. Baghaee, H.R., Mlakic, D., Nikolovski, S., Dragicevic, T.: Anti-islanding protection of PV-based microgrids consisting of PHEVs using SVMs. IEEE Trans. Smart Grid 11(1), 483–500 (2020)
43. Manikonda, S.K.G., Gaonkar, D.N.: Islanding detection method based on image classification technique using histogram of oriented gradient features. IET Gener., Transm. Distrib. 14(14), 2790–2799 (2020)
44. Liu, F., Zhang, Y., Xue, M., Lin, X., Kang, Y.: Investigation and evaluation of active frequency drifting methods in multiple grid-connected inverters. IET Power Electron. 5(4), 1–8 (2012)
45. Vahedi, H., Karrari, M.: Adaptive fuzzy Sandia frequency-shift method for islanding protection of inverter-based distributed generation. IEEE Trans. Power Delivery 28(1), 84–92 (2013)
46. Reigosa, D., Briz, F., Charro, C.B., Garcia, P., Guerrero, J.M.: Active islanding detection using high-frequency signal injection. IEEE Trans. Ind. Appl. 48(5), 1588–1597 (2012)
47. Bei, T.: Accurate active islanding detection method for grid-tied inverters in distributed generation. IET Renewable Power Gener. 11(13), 1633–1639.
48. Reigosa, D.D., Briz, F., Charro, C.B., Guerrero, J.M.: Islanding detection in three-phase and single-phase systems using pulsating high-frequency signal injection. IEEE Trans. Power Electron. 30(12), 6672–6683 (2015)
49. Xiao, H.F., Fang, Z., Xu, D., Venkatesh, B., Singh, B.: Anti-islanding protection relay for medium voltage feeder with multiple distributed generators. IEEE Trans. Ind. Electron. 64(10), 7874–7885 (2017)
50. Liu, M., Zhao, W., Wang, Q., Huang, S., Shi, K.: An irregular current injection islanding detection method based on an improved impedance measurement scheme. Energies 11(9), 1–18 (2018)
51. Operating manual Sunny Highpower PEAK3. www.files.sma.de/downloads/SHP-20-BE-en-14.pdf (2022). Accessed 1 July 2022

52. Wang, X., Freitas, W., Dinavahi, V., Xu, W.: Investigation of positive feedback anti-islanding control for multiple inverter-based distributed generators. IEEE Trans. Power Syst. 24(2), 785–795 (2009)
53. Samui, A., Samantaray, S.R.: New active islanding detection scheme for constant power and constant current controlled inverter-based distributed generation. IET Gener., Transm. Distrib. 7(7), 779–789 (2013)
54. Bakhshi-Jafarabadi, R., Ghazi, R., Sadeh, J.: Power quality assessment of voltage positive feedback based islanding detection algorithm. J. Modern Power Syst. Cleaner Energy 8(4), 787–795 (2020)
55. Bakhshi-Jafarabadi, R., Sadeh, J.: New voltage feedback-based islanding detection method for grid-connected photovoltaic systems of microgrid with zero non-detection zone. IET Renewable Power Gener. 14(10), 1710–1719 (2020)
56. Sivadas, D., Vasudevan, K.: An active islanding detection strategy with zero nondetection zone for operation in single and multiple inverter mode using GPS synchronized pattern. IEEE Trans. Ind. Electron. 67(7), 5554–5564 (2020)
57. Kaewthai, S., Ekkaravarodome, C., Jirasereeamornkul, K.: Novel disturbance and observation based active islanding detection for three-phase grid-connected inverters. J. Power Electron. 21(2), 438–450 (2021)
58. Bakhshi-Jafarabadi, R., Popov, M.: Hybrid islanding detection method of photovoltaic-based microgrid using reference current disturbance. Energies 14(5), 1–15 (2021)
59. Barkat, F. et al.: Hybrid islanding detection technique for single-phase grid-connected photovoltaic multi-inverter systems. IET Renewable Power Gener. 14(18), 3864–3880 (2020)
60. Rostami, A., Jalilian, A., Zabihi, S., Olamaei, J., Pouresmaeil, E.: Islanding detection of distributed generation based on parallel inductive impedance switching. IEEE Syst. J. 14(1), 813–823 (2020)
61. Serrano-Fontova, A., Martinez, J.A., Casals-Torrens, P., Bosch, R.: A robust islanding detection method with zero-non-detection zone for distribution systems with DG. Int. J. Elect. Power Energy Syst. 133, 1–16 (2021)
62. Bakhshi-Jafarabadi, R., Sadeh, J., Popov, M.: Maximum power point tracking injection method for islanding detection of grid-connected photovoltaic systems in microgrid. IEEE Trans. Power Delivery 36(1), 168–179 (2021)
63. Bakhshi-Jafarabadi, R., Sadeh, J., Chavez, J.d.J., Popov, M.: Two-level islanding detection method for grid-connected photovoltaic system-based microgrid with small non-detection zone. IEEE Trans. Smart Grid 12(2), 1063–1072 (2021)
64. Murugesan, S., Murali, V., Daniel, S.A.: Hybrid analyzing technique for active islanding detection based *d*-axis current injection. IEEE Syst. J. 12(4), 3608–3617 (2018)
65. Momesso, A.E.C., Kume, G.Y., Rodrigues Faria, W., Pereira, B.R., Asada, E.N.: Automatic recloser adjustment for power distribution systems. IEEE Trans. Power Delivery 1–10 (2022). https://doi.org/10.1109/TPWRD.2022.3141928
66. Saeedian, M., Pournazarian, B., Taheri, S., Pouresmaeil, E.: Provision of synthetic inertia support for converter-dominated weak grids. IEEE Syst. J. 16(2), 2068–2077 (2021)
67. Hansen, A.D., Das, K., Sørensen, P., Singh, P., Gavrilovic, A.: European and Indian grid codes for utility scale hybrid power plants. Energies 14(14), 1–15 (2021)
68. Demoulias, C.S. et al.: Ancillary services offered by distributed renewable energy sources at the distribution grid level: an attempt at proper definition and quantification. Appl. Sci. 10(20), 1–36 (2020)
69. Hassan, Z., Amir, A., Selvaraj, J., Rahim, N.A.: A review on current injection techniques for low-voltage ride-through and grid fault conditions in grid-connected photovoltaic system. Sol. Energy 207, 851–873 (2020)
70. Manikonda, S.K.G., Gaonkar, D.N.: Islanding detection method based on image classification technique using histogram of oriented gradient features. IET Gener. Transm. Distrib. 14(14), 2790–2799 (2020)
71. Dietmannsberger, M., Grumm, F., Schulz, D.: Simultaneous implementation of LVRT capability and anti-islanding detection in three-phase inverters connected to low-voltage grids. IEEE Trans. Energy Convers. 32(2), 505–515 (2017)
72. Zhang, C., Xu, Y.: Hierarchically-coordinated Voltage/VAR control of distribution networks using PV inverters. IEEE Trans. Smart Grid 11(4), 2942–2953 (2020)
73. Brandao, D.I., Ferreira, W.M., Alonso, A.M.S., Tedeschi, E., Marafao, F.P.: Optimal multiobjective control of low-voltage AC microgrids: power flow regulation and compensation of reactive power and unbalance. IEEE Trans. Smart Grid 11(2), 1239–1252 (2020)
74. Gómez-Expósito, A., Conejo, A.J., Cañizares, C.A.: Electric Energy Systems: Analysis and Operation. 2nd Ed., Boca Raton Boca Raton, FL (2020)
75. Kontis, E.O., del Nozal, A.R., Mauricio, J.M., Demoulias, C.S.: Provision of primary frequency response as ancillary service from active distribution networks to the transmission system. IEEE Trans. Smart Grid 12(6), 4971–4982 (2021)
76. ENTSO-E assesses the impact of reduction of inertia on frequency stability in long-term scenarios. European Network of Transmission System Operators for Electricity (2021). Accessed 6 December 2021
77. Shi, K. et al.: Transient analysis of microgrids with parallel synchronous generators and virtual synchronous generators. IEEE Trans. Energy Convers. 35(1), 95–105 (2020)
78. Rakhshani, E., Rodriguez, P.: Inertia emulation in AC/DC interconnected power systems using derivative technique considering frequency measurement effects. IEEE Trans. Power Syst. 32(5) 3338–3351 (2017)
79. Shi, K., Ye, H., Xu, P., Yang, Y., Blaabjerg, F.: An islanding detection based on droop characteristic for virtual synchronous generator. Int. J. Elect. Power Energy Syst. 123, 1–9 (2020)
80. Shukla, A., Dutta, S., Sadhu, P.K.: An island detection approach by $\mu$-PMU with reduced chances of cyber attack. Int. J. Elect. Power Energy Syst. 126, 1–12 (2021)
81. Installation manual Sunny Tripower 60. www.files.sma.de/downloads (2022). Accessed 1 July 2022
82. Manual of Kaco blueplanet 87–165 TL3. www.kaco-newenergy.com/products/blueplanet-125-TL3-165-TL3 (2022). Accessed 1 July 2022

**How to cite this article:** Bakhshi-Jafarabadi, R., Sadeh, J., Serrano-Fontova, A., Rakhshani, E.: Review on islanding detection methods for grid-connected photovoltaic systems, existing limitations and future insights. IET Renew. Power Gener. 1–16 (2022). https://doi.org/10.1049/rpg2.12554